Effect of Strain Rate on Tensile Fracture Behaviour of Viscoelastic Matrix (EPOXY) and Fiber Reinforced Composites

Mashaan Ibrahem Hassan Arz Yahya Rzayeg Saad Mohamed Jaleel
University of Al- Anbar - College of Engineering

ABSTRACT
Viscoelasticity, as its name implies, is a generalization of elasticity and viscosity. Many industrial applications use viscoelastic matrix with reinforcement fiber to obtained better properties. Tensile testing of matrix and one types of fabric polyamide composites was performed at various loading rates ranging from ($8.16* 10^{-5}$ to $11.66 * 10^{-5}$ m/sec) using a servohydraulic testing apparatus. The kind of reinforcement, random glass fiber (RGF), and the kind of matrix, epoxy (E) are used shown that the linear strain (≤ 0.5) for the three parameter model gives a good agreement with experimental results. The results showed that both tensile strength and failure strain of these matrices and composites tend to decrease with increase of strain rate. The experimental results were comparison with numerical results by using ANSYS 5.4 program for simple study case has shown some agreement. Fracture regions of the tested specimens were also observed to study micro mechanisms of tensile failure.

KEYWORDS:
tensile behavior, polyamide composite, strain rate dependence, fiber viscoelastic.

تأثير معدل الانفعال على معامل الكسر للمواد المركبة من مواد مرنة لزجة (ايبوكسي) وألياف رابطة

مشعان إبراهيم حسن و أرز يحيى رزيك و سعد محمد جليل

الخلاصة:

المادة التي يتضمن تكوينها مادتين إحداهما مرنة والأخرى لزجة يطلق عليها مصطلح المواد المرنة اللزجة. يستعمل في العديد من التطبيقات الصناعية ألياف التقوية مع المواد المرنة اللزجة للحصول على أفضل الخواص. لقد تم أجراء دراسة عملية استخدام فيها جهاز اختبار الشد الهيدروليكي أولا للمادة الرابطة والمتمثلة بالمادة المرنة اللزجة (ايبوكسي) وثانيا للمادة المتراكبة والتي استخدم فيها نفس المادة الرابطة. الألياف المستخدمة هي الألياف العشوائية الزجاجية وتم الاختبار عند نسب تحيل مختلفة يتراوح من(٨.١٦ * ١٠ $^{-٥}$ م/ثانية) إلى(١١.٦٦ * ١٠ $^{-٥}$ م/ثانية). بينت النتائج إن هناك تقارب ملحوظ بين النتائج العملية و البرنامج المتطور والمتمثل بالنموذج ذو المعاملات الثلاثة وخصوصا في حالة كون الانفعالات الخطية التي اقل من (٠.٥).وتبين النتائج إن معامل المرونة للمواد المرنة اللزجة والمواد المتراكبة متزايد بزيادة كلا من معدل الانفعال والزمن. كما تمت مقارنة النتائج العملية مع النتائج العددية باستخدام برنامج(**ANSYS 5.4**) لبعض الحالات البسيطة والتي أعطت توافق كبير .مناطق كسر النماذج المُجرّبةِ لوحظتْ أيضاً لدِراسَة الآلياتِ الدقيقةِ فيْ الفشلِ أثناء اختبار الشدِّ.

1. INTRODUCTION

In practical engineering design, strains and stresses are very important criteria in reliability and serviceability evaluations of structures. Viscoelasticity is an important concept for determining long – time behaviour (service-life time) of structures. Viscoelasticity permits us to describe the behaviour of materials exhibiting strain rate effects under applied loads. These effects are illustrated by creep phenomena under certain loads or by stress relaxation under a constant deformation. For most composites, the viscoelastic behaviour is primarily due to the matrix. Composite materials are reinforced with fibers in part to resist creep deformation. The magnitude of the creep deformation induced in a composite structure under a certain loading is influenced by a variety of some factors, such as material architecture, temperature, humidity, loading frequency, and stress level [1]. Tensile testing of continuous fiber reinforced polymer composites has been performed to characterize the tensile mechanical behaviour of the composites. Mechanical properties such as elastic modulus were obtained by using tensile testing systems [2]. The assumptions used are that the matrix is linear viscoelastic and the fibers are elastic. The viscoelastic analysis techniques may broadly be classified into three approaches, viz. (i) quasi-elastic solutions, (ii) integral transform techniques, and (iii) direct methods. Quasi-elastic solution uses elastic properties equivalent to the corresponding viscoelastic properties at the desired time and temperature. This approach essentially ignores the entire past history of loading and environment and therefore yields gross approximation to the true response. Integral transform technique [3] is based on the corresponding principle, in which using the elastic solution, the corresponding viscoelastic solution is obtained using Laplace transform technique. This approach is exact for which closed form solutions are possible and approximate Laplace transform inversion has to be employed for the problems with the numerical elastic solution [4]. Further, the transform technique is not directly applicable for the problems of non-homogeneous transient temperature distributions. To circumvent these problems, conditions of constant temperature over time increments are imposed and the correspondence principle is applied on an incremental basis [5]. The direct formulations are based on the finite element theory using either the differential form [6] or the integral form [7] of stress-strain relationships.

In this work studying the behaviour of one matrix is used and random glass fiber (RGF) of composite beams. Package program (***ANSYS 5.4***) are used in this work to compression between experimental results with numerical results for these four types of composite beam at greatest load used and studying new cases illustrated the viscoelastic composite behaviour.

It is well known that the straightforward application of the displacement method to nearly incompressible structures yields erratic displacements and severely oscillating stresses about the exact solution and across the elements. This aspect has been studied for elastic materials and is well documented in literature [8]. The remedies suggested in literature to overcome the difficulties are the use of: (i) refined meshes, (ii) reduced Poisson's ratio, (iii) alternate formulations. Such as the stress hybrid approach and the formulation based on Hermann's (Semi-Reissner's) variational principle, and (iv) reduced integration for the troublesome portion of the strain energy. The proposition of mesh refinement [9] needs number of elements and yields doubtful results and therefore is not advisable. The results obtained using the reduced Poisson's ratio have to be extrapolated so as to obtain the results corresponding to the required Poisson's ratio [10].

2. VISCOELASTIC MODEL

The mechanical model is equivalent to describe the viscoelastic behavior and construct of elastic spring, this will obey Hooke's laws, and viscous dashpots, which obey Newton's law of viscosity [11].

The simplest mechanical model is a combination of one spring with one dashpot linked either in parallel (Voiget or Kelvin model) or in series (Maxwell model) [12]. Each spring element is assigned a stiffness (E), which represents modulus of elasticity, and each dashpot is assigned a frictional resistant (force-velocity of displacement), λ which represent the viscosity [13].

The two models couldn't satisfy the viscoelastic properties (creep and relaxation) completely if they are used alone, the combination between two models (Maxwell- Kelvin model) gives good results in both creep and relaxation [14].

2.1 Maxwell Model

A spring and dashpot in series, as shown in **Fig .(1)**, form this model. For simple tension as σ_o is applied at t = 0, an immediate elastic strain ε^e of the spring occurs. Then a viscous strain ε^v of dashpot is added. The total strain is equal to the sum of the strain in each component. While the stress acts on them is the same. The total strain can be written as:

$$\varepsilon = \varepsilon^e + \varepsilon^v \tag{1}$$

Then the strain rate is:

$$\frac{d\varepsilon}{dt} = \frac{d\varepsilon^e}{dt} + \frac{d\varepsilon^v}{dt} \tag{2}$$

Thus, the governing equation of Maxwell model is [12]:

$$\frac{d\varepsilon}{dt} = \frac{1}{E} \bullet \frac{d\sigma}{dt} + \frac{\sigma}{\lambda} \tag{3}$$

It is of interest to examine the response of such a material to various stress and strain histories. In the case of the application of constant stress, eq.(3) is reduced to:

$$\frac{d\varepsilon}{dt} = \frac{\sigma}{\lambda} \tag{4}$$

then by integration,

$$\varepsilon = \frac{\sigma t}{\lambda} + \frac{\sigma_o}{E} \tag{5}$$

Eq.(5) explains that only viscous flow is observed with time. After the time t_1, the stress σ is removed; an immediate recovery of elastic component of strain occurs leaving irreversible strain of viscous element as shown in **Fig.(2)**. For the case of constant strain as shown in **Fig.(2)**, eq.(3) will be:

$$\frac{d\sigma}{\sigma} = \frac{-E}{\lambda} dt \tag{6}$$

by integration,

$$\sigma = \sigma_o \exp\left(\frac{-t}{t'}\right) \tag{7}$$

Where ($t' = \lambda / E$) is the 'relaxation time'.**Fig.(2)** shows the creep and recovery, stress relaxation for Maxwell models [12].

2.2 Voiget Or Kelvin Model

This model consists of spring and dashpot in parallel as shown in **Fig. (3)**. As σ_o applied, a dashpot prevents an instantaneous extension of the elastic spring. With time, the viscous behavior causes an increase of the strain. The total strain, elastic strain, and the viscous strain are equal, and each component supports a portion of σ_o. therefore:

$$\sigma_o = \sigma = \sigma^e + \sigma^v \tag{8}$$

$$\sigma = E\varepsilon + \lambda \frac{d\varepsilon}{dt} \tag{9}$$

Beginning with the creep, where the model supports to constant stress, the solution of governing eq.(9) is:

$$\varepsilon = \frac{\sigma_o}{E}\left[1 - \exp(\frac{-t}{t''})\right] \tag{10}$$

Where $t'' = \lambda / E$ is the retardation time.

Comparison eq.(10) and eq.(5) indicate that, the predicted creep behavior of the Kelvin model is more realistic, since the strain approaches to σ_o / E as time approaches infinity [17]. The response of Kelvin model to constant load is most readily understood by considering the recovery response, where $\sigma = 0$, then

$$E\varepsilon + \lambda \frac{d\varepsilon}{dt} = 0 \tag{11}$$

By integration:

$$\varepsilon = \varepsilon_o \exp(\frac{-t}{t''}) \tag{12}$$

Fig.(4) shows the creep and recovery behavior of Kelvin model. Consider now Kelvin model subjected to constant strain as shown in **Fig.(4)**, then eq.(9) will be reduced to:

$$\sigma = E\varepsilon \tag{13}$$

Eq.(13) implying that the material behaves as an elastic solid which is an dequate for general viscoelastic behavior [15]. It is shown that Maxwell model gives a reasonable prediction of relaxation but it has unlimited deformation, whereas, Kelvin models provide a better prediction for creep and recovery but it provides for a maximum displacement limited by the elastic deformation of the spring [16].

We used in this study the another simple and more general than Maxwell or Kelvin model is the standard linear solid, which is formed by the combination of Maxwell and Kelvin model as shown in **Fig.(5)**. It exhibits an instantaneous glassy response as well as delayed elasticity and recovery [17]. **Fig.(6)** shows the creep, recovery and stress relaxation of the standard linear solid, which are more realistic than Maxwell or Kelvin model.

The shear relaxation modulus and creep compliance of shear stress is shown in **Fig.(5a)**.

$$G(t) = E_o + E_1 e^{-t/t_1}, \tag{14a}$$

Where: $t_1 = \lambda_1 / E_1$,

$$J(t) = \frac{1}{E_o} - \frac{E_1}{E_o(E_o + E_1)} e^{-t/t_2} \tag{14b}$$

Where: $t_2 = E_1 E_2 / \lambda_1$,

While the shear relaxation modulus and creep compliance of **Fig.(5b)** is shown below,

$$G(t) = \frac{E_1 E_o}{E_1 + E_o} + \frac{E_o^2}{E_1 + E_o} e^{-t/t_1} \tag{15a}$$

Where: $t_1 = (E_o + E_1) / \lambda_1$,

$$J(t) = \frac{1}{E_o} + \frac{1}{E_1}\left(1 - e^{-t/t_2}\right) \tag{15b}$$

Where: $t_2 = \lambda_1 / E_1$,

The behavior of these models under on entirely different set of condition provides a reasonable predication of real materials [16].

3. SHEAR ELASTIC MODULUS

It will be necessary to describe the definition and measurement of the parameter is used to quantify viscoelastic effects. Experimental work gives the shear elastic modulus by using the tensile test for (E). By using the curve fitting program can be obtained to the coefficient of the shear relaxation. This program used the last square method to solve the polynomial equation. **Fig.(7)** show that the comparison between the experimental results with the results of the curve fitting program (prony series) for the shear elastic modulus with the time. All constant parameters of the viscoelastic material are as shown in the following **Table.(1)**. The rheological model is the Generalized Kelvin and Maxwell model in deviatoric component and elastic in volumetric component as shown in **Fig.(8)**.

4. EXPERIMENTAL PROCEDURE

4.1 Material And Specimen

Random glass fiber (RGF) polyamide composites were studied in this work. This random fiber was used as the reinforcement in these composites. The matrix was epoxy (E). It is known that (E) has higher stiffness and strength than polyester (P). The composites are denoted here after by RGF/E. The fiber volume fractions were 48% for RGF/E at 8 layers and 32% for RGF/E at 9 layers. Tensile specimens were cut from the laminates and the direction of the warp threads corresponded with the tensile loading direction. Specimen geometry has shown in **Fig.(9)**.

5. RESULTS AND DISCUSSION

5.1 Tensile Testing

Stress-strain relations of (E) at three different loading rates are shown in **Fig.(10)**. For the polyamide composites the stress –strain relations obtained at the ($11.6* 10^{-5}$ m/sec) are shown in **Fig.(11)**. It has been postulated that the nonlinearly in random fabric composites is caused by micromechanical deformation such as shear deformation of the longitudinal threads, extensional deformation of the matrix regions and transverse cracking of the transverse thread. It is clearly seen from **Fig.(10)** and **Fig.(11)** that the nonlinear stress-strain behaviors in both epoxy matrix (E) and the random glass fiber (RGF) composites. Dependence of the initial tensile modulus on strain rate is shown in **Fig.(12)** and **Fig.(13)** respectively. The tensile module of E, and RGF/E tended to slightly increase as strain rate increased, while this modulus appeared decrease as time increased as shown in the **Fig.(14)** and **Fig.(15)** respectively.

5.2 Fracture Mechanism

RGF is used in this work show the photos in **Fig.(16)**. **Fig.(17)** show that the photos of the RGF/E composite before tensile test. Failure regions of the RGF/E composite at loading rate ($11.66 * 10^{-5}$ m/sec) are shown in **Figs.(18),(19)**.For RGF/E composite, a relatively straight fracture line perpendicular to the tensile direction and pull-outs of fiber bundles was observed. The damages such as matrix cracking, debonding, interfacial failure and delamination show that in **Figs.(18),(19)**.

6. NUMERICAL RESULTS

After making a preview for the experimental work, **Figs.(20)**,**(21)** shows the comparison between the experimental results for both model on the greatest load used for viscoelastic composite beam with the numerical solution for using **ANSYS 5.4** program the viscoelastic beam for the same geometry and characteristics. The general behavior of epoxy seems to be stable, though it is increasing slowly and clearly with the course of time. This can be seen clearly from the experimental results. **Fig.(20)** shows the behavior of the viscoelastic beam increases with the time, and this increasing continues with exceeding the limits of the viscoelastic composite beam. This figure differs from other figure, in general behavior. This difference returns to the magnitude of harmonic between the loads with the number of layers are used. **Fig.(21)** show that some how approximate results and shows a good agreement when compared with another figure above because the numbers of the layers with the applied load are harmonic.

7. CONCLUSIONS

1. Random E-glass fiber composite with epoxy matrix showed better tensile performance at all testing rates than epoxy matrix.
2. Epoxy matrix has shown very good fracture resistance. The tensile test shows that clearly and the ratio of epoxy matrix resistance against the effective load is excellent.
3. The tensile mechanical properties of RGF/E dramatically increased as strain rate increased. On the other hand, the elastic modulus of both matrixes only and composite decreased as strain rate increased and then slightly decreased at high strain rates. As a result, the elastic modulus in general increased as the strain rate increased.

REFERENCES

[1] J. S. Harris and E. J. Barbero "Prediction of Creep Properties of Laminated Composites from Matrix Creep Data" J. of Reinforced Plastics and Composites. 17(4): 361-378 (1998).
[2] K. Kawata ; S. Hashimoto and N. Takeda, In "Proc. 4th Int. Conf. On Composite Materials". ICCMIV, Eds T.Hayashi et al., Tokyo, 829-836 (1982).
[3] E. H. Lee, "Stress Analysis of Viscoelastic Bodies". Quart. Appl. Math. 13, 183-190 (1955).
[4] R. A. Schapary, "Approximate Methods of Transform Inversion for Viscoelastic Stress Analysis". Proc. 4th U.S. Nat. Cong. . Appl. Mech. 2, 1075-1085 (1962).
[5] H. H. Hiltion and R. G. Russel, "An Extension of Alfreys Analogy to Thermal Stress Problems in Temperature Dependent Linear Viscoelastic Media". J. Appl. Phys. Sci. 9, 152-164 (1961).
[6] W. C. Carpenter, "Viscoelastic Stress Analysis". Int. J. Num. Meth. Engng 4, 357-366 (1972).
[7] J. L. White, "Finite Elements in Linear Viscoelasticity". Proc. 2nd Conf. Matrix. Meth. Struct. Mech. AFFDLTR-150. 489-516 (1968).
[8] E. J. Hearn, "Mechanical of Materials", 1st edition, pergaman press, vol. (2), (1977).
[9] F. J. Lockett, "Non-Linear Viscoelastic Solids", Johnwiely & Sonsinc, New York, (1977).
[10] I. H. Hall, "Viscoelasticity", in cyclopedia of polymers & Engineering, vol. (17), (608-609), (1985).
[11] H. Assonnet, "Buckling Behavior of Imperfect Elastic & Linearly Viscoelastic Structures", Inc. J. Solids & Struct, vol. (74), No. (10), (755-784), (1974).
[12] S. J. Hearn., "Mechanics of Materials", 2nd edition pergaman, (1985).
[13] R. M. Christensen, "Theory of Viscoelasticity", 2nd edition.
[14] M. L. Williams, "Structural Analysis of Viscoelastic Materials", ALAA J., Vol. (2), NO. (5), May, (785-808), (1964).
[15] R. Herrmann. "Elasticity Equations for Incompressible and Nearly Incompressible Materials by a Variational Theorem". AIAA. J. 3, 1896-1900 (1965).
[16] I. M. Smith. "Incremental Numerical Solution of a Simple Deformation Problem in Soil Mechanics". Geotechnique 20. 357-372 (1970).
[17] Y. Huang." Finite Element Analysis of Non-Linear Soil Media". Application of Finite Elements in Civil Engineering. Pp. 663-690. Vanderbilt University (1969).

NOMENCLATURE

Symbol	Definition	SI Unit
d	Differential operator	---

(E)	Epoxy	---
E	Elastic modulus	$N.m^{-2}$
E_0,E_1,E_2	Young's modulus for spring in mechanical model	$N.m^{-2}$
F	Fiber	---
G(t)	Shear relaxation modulus	N.m-2
J(t)	Creep compliance	m2.N-1
t	Current time	Sec
t_1,t_i	Relaxation time	Sec
t_2,t_j	Retardation time	Sec
λ	Damping coefficient	---
σ	Normal stress	N.m-2
σ_o	Initial stress	N.m-2
σ^e	Elastic stress	N.m-2
σ^v	Viscous stress	N.m-2
ε	Normal strain	---
ε_o	Initial strain	---
ε^e	Elastic strain	---
ε^v	Viscous strain	---

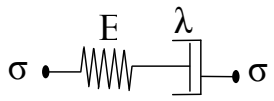

Fig. 1. Maxwell Model.

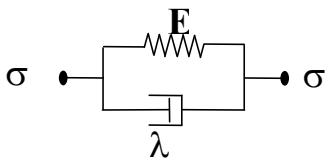

Fig. 3. Kelvin Model.

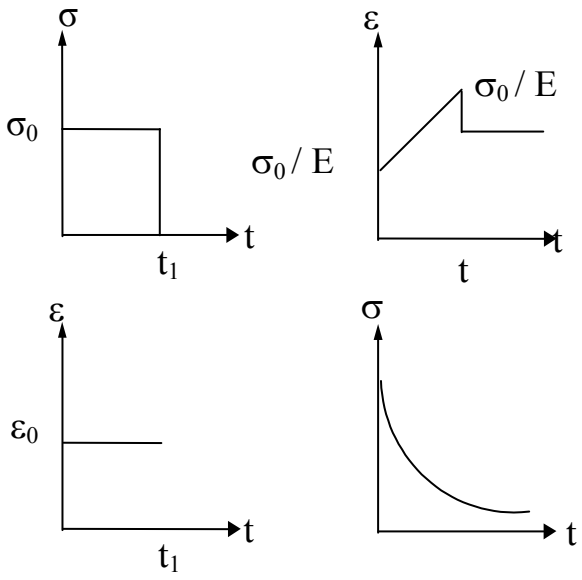

Fig. 2. Creep and Recovery of Maxwell Model.

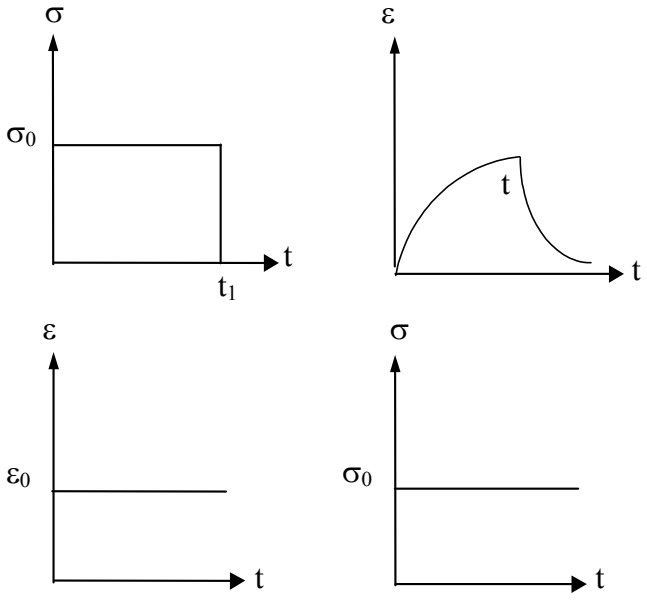

Fig. 4. Creep, Recovery & Relaxation Behavior of Kelvin Models.

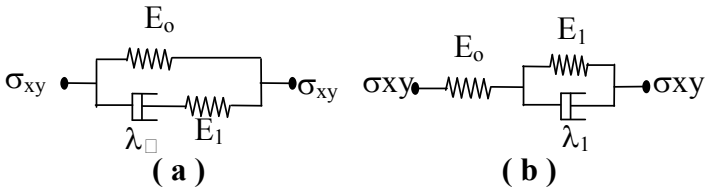

Fig. 5. Standard Linear Solid Model.

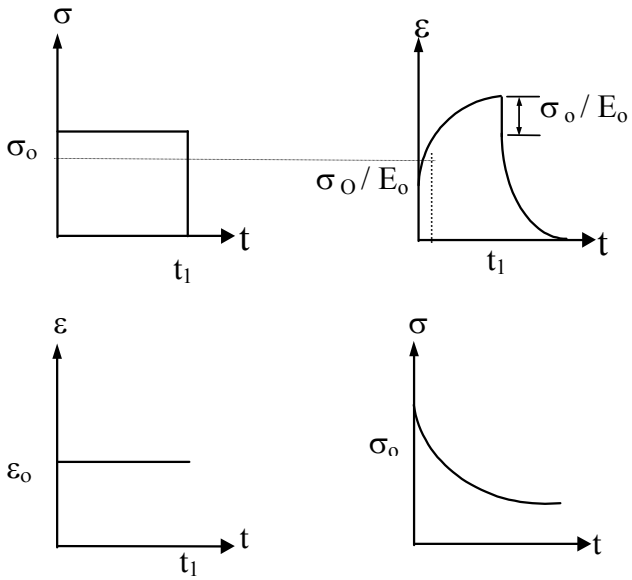

Fig. 6. Creep, Recovery & Relaxation Behavior of Standard Linear Solid

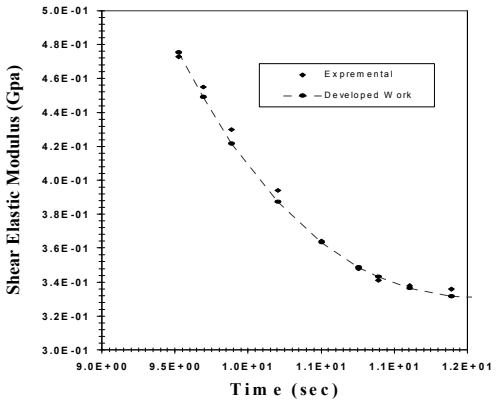

Fig.7. Shear elastic modulus of (E).

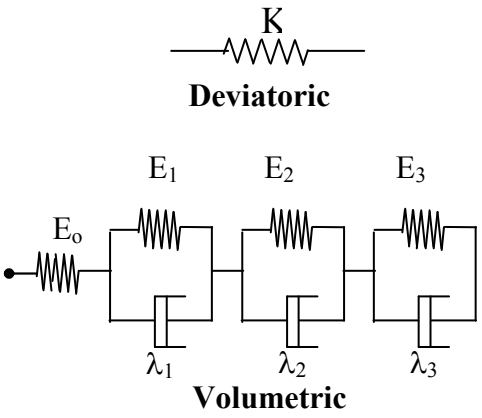

Fig .8. Generalized Kelvin and Maxwell model.

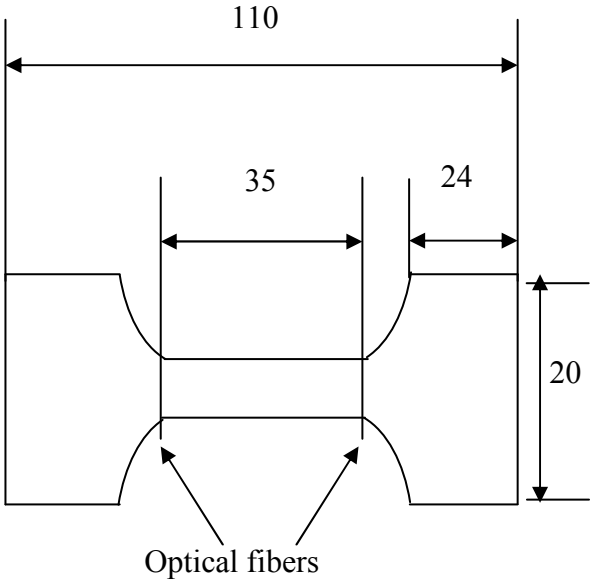

Fig. 9. Tensile specimen geometry.

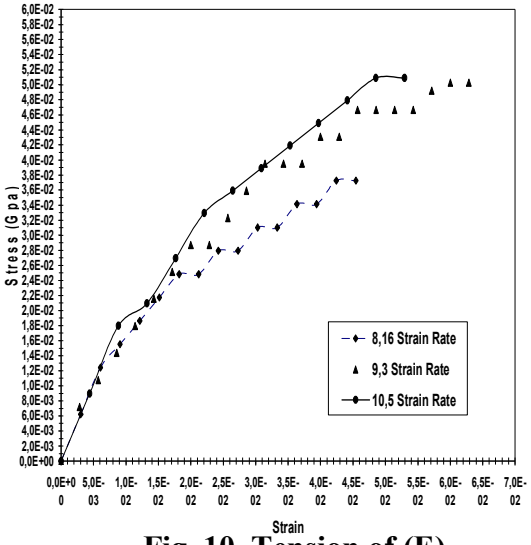

Fig. 10. Tension of (E).

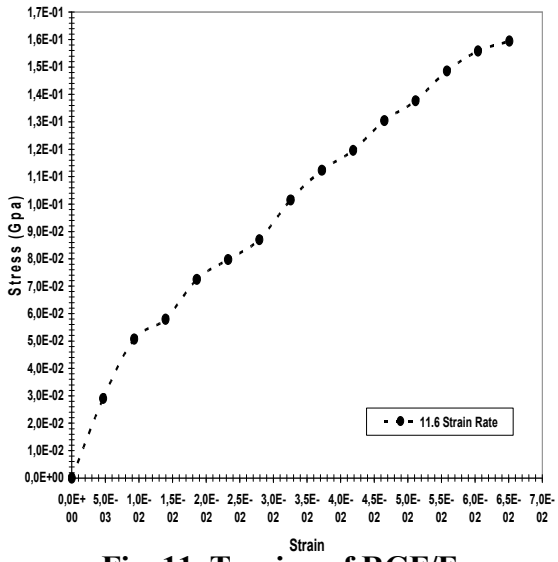

Fig. 11. Tension of RGF/E.

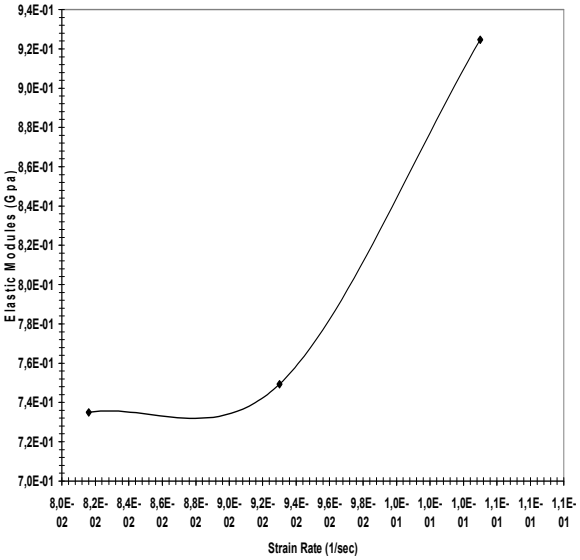

Fig. 12. Elastic modules vs. Strain Rate of (E).

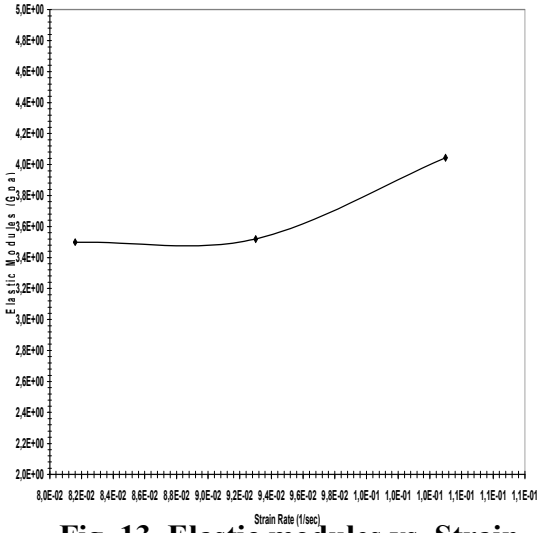

Fig. 13. Elastic modules vs. Strain Rate of RGF/E.

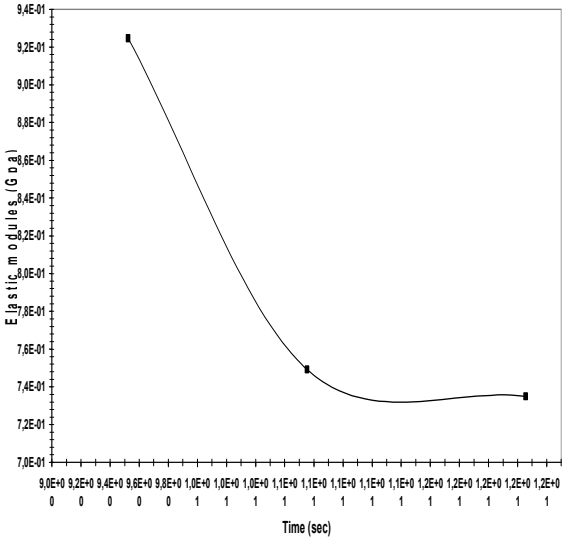

Fig. 14. Elastic modules vs. Time of (E).

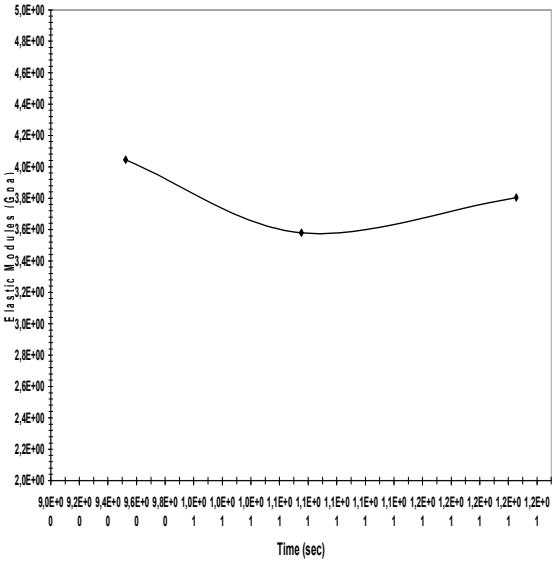

Fig. 15. Elastic modules vs. Time of RGF/E.

Fig. 16. RGF is used.

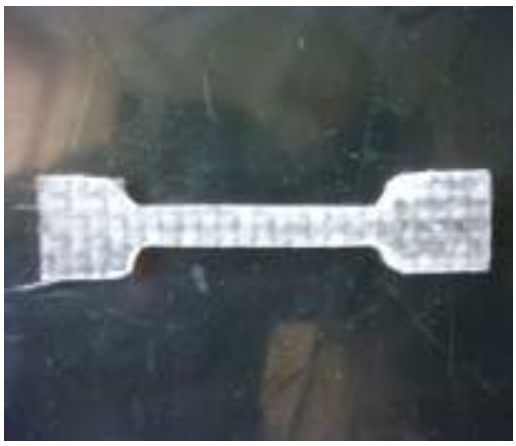

Fig. 17. RGF/E before test.

Fig. 18. RGF/E after test.

Fig. 19. RGF/E after test.

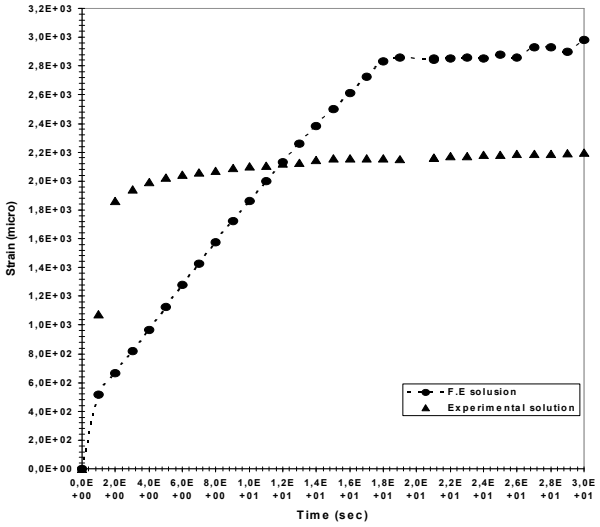

Fig. 20. Comparison between viscoelastic composite RGF/E (8 layer) with viscoelastic (E) at (9 N).

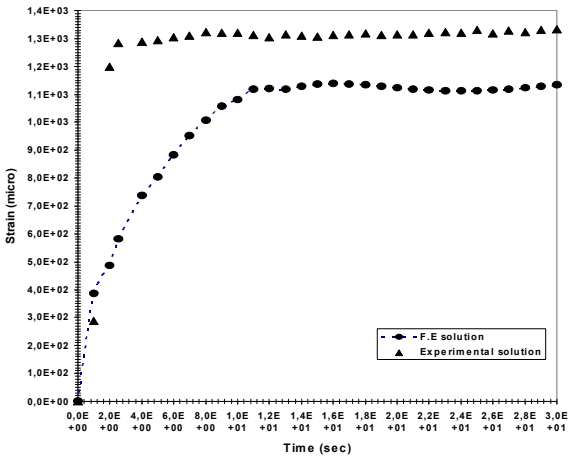

Fig. 21. Comparison between viscoelastic composite RGF/E (9 layer) with viscoelastic (E) at (19 N).

Table.1 Explain the Experimental Coefficient of the Shear Relaxation.

E0	E1	E2	E3
-24.269	1.001 E05	-2.88 E05	1.879 E05
λ1	λ2	λ3	K
0.095	0.093	0.091	0.295 E09